NASA TECHNICAL MEMORANDUM

NASA TM X-67922

NASA TM X-67922

BEAM FOCUSING CHARACTERISTICS OF VARIOUSLY SHAPED GRID HOLES

by David C. Byers and Bruce A. Banks
Lewis Research Center
Cleveland, Ohio
September 1971

This information is being published in preliminary form in order to expedite its early release.

BEAM FOCUSING CHARACTERISTICS OF VARIOUSLY SHAPED GRID HOLES

by David C. Byers and Bruce A. Banks

Lewis Research Center

SUMMARY

Tests were made to determine the ion focusing characteristics of circular, hexagonal, square, and triangular screen grid holes. The focusing was found to be dependent on both the thruster operating conditions and the screen grid hole shape and size. The circular hole shape had the lowest erosion ratios followed in increasing order by the hexagonal, square, and triangular shapes. The hexagonal hole shape appeared to be the most promising noncircular shape for high open area grids. Inspection of the erosion patterns provided a correlation between the shapes of the screen grid holes and the ion beamlet shape in the region of the accelerator grid. This correlation was used to produce square ion beamlets which could be of interest for an electrostatic beam deflection scheme. The effect of various defects in the screen grid was also investigated.

E-6558

INTRODUCTION

The electron-bombardment ion thruster is being considered for a variety of space missions (refs. 1, 2, and 3) for which the optimum specific impulse is between 2000 to 3000 seconds. As the specific impulse decreases, the discharge energy required per beam ion (eV/ion) becomes an increasingly important loss mechanism. It is well known (refs. 4 and 5) that the eV/ion decreases as the open area fraction of the screen grid increases. Bechtel (ref. 4) has found, for example, that as the open area fraction of the screen grid was increased from 0.48 to 0.75, the eV/ion (at 0.8 propellant utilization) decreased from about 550 to 250.

The standard thruster grid configuration has consisted of a hexagonal array of circular holes in both the screen and accelerator grids. The maximum open area fraction for a hexagonal array of circular holes is 0.906, which occurs when the minimum web distance is zero. Larger open area fractions can be obtained with arrays of hexagonal, square, or triangular holes if the web thicknesses are made equal to that of hexagonal arrays of circular holes. Grids with such hole shapes might then provide improved discharge chamber performance. In addition, electrostatic beam deflection schemes are presently being studied (ref. 6) for thrusters sized for satellite station-keeping applications. It is possible that screen grid hole shapes other than circular could provide optimum beam deflection characteristics.

This paper presents the results of a preliminary study of the ion focusing characteristics of screen grid holes of various shapes. The investigation included variation of both the ion beam current and the extraction voltages. The impact on ion focusing of certain irregularities in screen grid holes was also determined.

APPARATUS AND PROCEDURE

The 30-cm thruster with which the tests were made was nearly identical to the Task I thruster of reference 7. The screen grid was 1.52 mm thick with 5.0 mm holes drilled on a 5.6 mm center-to-center spacing. The accelerator grid was 2.0 mm thick with 4.0 mm diameter holes.

The screen grid hole shapes to be tested were electric-discharge machined into 0.13 mm thick tantalum sample sheets about 3.8 cm in diameter. The number of holes machined into the sample sheet was such as to surround the central hole with holes in a regular pattern. The sample sheets were placed on the upstream side of the screen grid over four large open areas. The central hole in each sample was at a radius of 7 cm from the thruster axis. Solid tantalum sheets between 0.05 and 0.13 mm thick were then placed on the upstream side of four matching areas cut into the accelerator grid. Ions extracted by the holes in the screen sample plate then impinged on the sheets on the accelerator grid and sputtered through in about one-half hour. Figure 1 shows an upstream view of the assembled accelerator and screen grids after a test. The edges of the holes machined into the screen grid sample sheets can be faintly seen. The shapes of the holes sputtered through the accelerator grid sample sheets can be seen clearly because their dimensions are smaller than those of the holes in the screen grid samples. The shapes of the hole patterns eroded on the accelerator grid samples were assumed to be representative of the focusing characteristics of the corresponding screen grid holes.

The dimensions of the sample holes presented herein were obtained with photographs which were taken at 10× magnification. All tests were run in a 1.5 m diameter, 4.5 m long, vacuum facility. Operating pressures were about 7×10^{-6} torr during all tests.

RESULTS AND DISCUSSION

The ion focusing characteristics of circular, hexagonal, square, and triangular holes are given at several values of initial grid spacing and ion beam current. Some operating parameters during the tests are shown in table I. The length, L, given on table I was the measured grid-to-grid spacing plus the screen grid hole sample thickness. The grid spacing was measured before and after the tests and agreed to within about 7 percent. The grid-to-grid spacing probably changed during thruster

operation. The extent of such variation was, however, not known.

Test I

Only the circular screen hole sample was placed on the screen grid for this test. The ion focusing characteristic of circular holes are quite well known over a large range of ion beam current and extraction voltages (refs. 8 and 9).

The circular hole screen grid sample is shown in figure 2(a). The diameter of the holes was about 5 millimeters, which was the diameter of the holes in the standard screen grid. Thus, the ion current per hole was about equal for the holes in the screen grid samples and in the standard screen grid.

Figure 2(b) shows the holes eroded on the accelerator grid sample after about 1 hour of operation. Figure 2(b) shows that the holes, although somewhat irregular, were roughly circular. As with all accelerator grid samples presented herein, the ion bombardment led to an area sputtered clear through surrounded by a fringe area where the ion sputtering was less intense. The fringe areas are seen in figure 2(b) as the light rings surrounding the holes. Ultimately, the metal within the fringe area would probably erode completely through. Therefore, the dimensions listed herein for the extent of erosion of the accelerator grid samples include the fringe region.

It was assumed herein that after a few hours of operation the fringe areas were representative of the erosion patterns after long-term operation. It is possible that the shape of the holes eroded in the accelerator grid sample could affect the ion focusing characteristics. If this were true the shape of the hole could change continuously with time. Such a situation could only be determined by long duration testing which was beyond the scope of this program. This situation has, however, not been found to exist during long duration tests of circular holes.

The erosion of the holes on the accelerator grid samples was observed visually during the test. The locations of maximum erosion within each beamlet could be determined because these locations would erode through first and were illuminated by the discharge plasma. In addition, the small areas of accelerator grid sample opposite the holes in the screen grid sample holes would fall off during the test and areas of erosion could be determined after the test. Sketch A shows the upstream accelerator face for the circular hole screen grid sample of Test I and a section view of the accelerator grid sample in the region of a single hole pattern which has not yet sputtered through. The dark areas indicate regions of maximum sputtering. The beamlets for a hexagonal array of circular holes appeared to have a second order hexagonal shape with maximum current density along the edge of the hexagon. The current density variation within each beamlet appears to be dependent on both the

shape and arrangement of the screen apertures.

One figure of merit for evaluating the ion focusing of various hole shapes is the ratio of the average dimension of the sputtered area (including the fringe) on the accelerator sample to the dimension of the hole in the screen grid. This ratio will be referred to as the erosion ratio. For the azimuthally symmetric circular hole case the erosion ratio is merely the ratio of the diameter or radius of erosion on the accelerator grid to the corresponding dimension of the screen grid hole. The dimensions selected to determine the erosion ratios are shown on sketch (B). For Test I the erosion ratio was 0.45. The characteristic dimensions used to specify the erosion ratios for all tests are shown on sketch B and tabulated in table II. To insure performance flexibility, the accelerator aperture dimensions should be somewhat larger than the dimension of the fringe areas on the accelerator grid sample - even though small accelerator holes improve thruster performance (ref. 10). Because of grid lifetime considerations screen grid aperture geometries which produce high erosion ratios would probably limit performance flexibility. Any mode of grid operation which causes the sputtered areas on the upstream face of the accelerator grid to connect between adjacent accelerator apertures would lead to early grid failure.

Test II

Circular, hexagonal, square, and triangular holes were tested simultaneously in Test II in the configuration shown in figure 1. The latter three screen grid samples are shown in figures 3(a), (b), and (c), respectively. The circular sample was that shown in figure 2(a). Two characteristic dimensions were selected to specify the erosion ratios for the noncircular samples. The distance from the sample center of symmetry to a side is specified as R_S or R_A on the screen or accelerator sample, respectively. The distance from the center of symmetry to the intersection of sample corners is called D_S and D_A. These dimensions are shown in sketch B. The characteristic dimensions of the hexagonal and square samples were about the same as for the circular sample. The triangular holes were made somewhat larger than the other samples due to a fabrication error.

Thrusters are typically operated over a range of ion beam currents which represent fraction of Child's law in current somewhat larger than that of Test I. It was thus desirable to determine the effect of operation at increased fraction of Child's law ion current on ion focusing characteristics. To increase the Child's law fraction, several operating parameters were changed from Test I: The total extraction voltage was decreased from that of Test I by 250 volts, the ratio of net (screen) to total (screen plus accelerator) voltage was decreased from 0.75 to 0.62, the ion beam current was increased from 0.42 to 0.54 amperes, and the grid spacing was increased by about 0.6 mm.

The beamlet current density variations for the hexagonal, square, and triangular shaped screen holes were determined in a manner similar to the circular holes of Test I and are shown in sketches C, D, and E, respectively. The sketches show where the slots first appeared in the accelerator grid samples prior to complete erosion. In each polygon hole, the slots first appeared at the bisection of the interior angles.

The accelerator grid samples produced from the circular, hexagonal, square, and triangular screen hole shapes are shown in figures 3(d) to (g), respectively.

Circular holes. - As seen in table II and by comparison of figures 2(b) and 3(d), the change in thruster operating conditions during Test II increased the dimensions of the erosion over those of Test I by about 11 percent. The ion focusing properties are thus a relatively strong function of the thruster operating conditions. With the exception of small random irregularities, the erosion patterns for all the central and peripheral circular holes were nearly identical. This indicated, as mentioned previously, that the erosion was primarily a function of the individual hole boundary and that the surrounding holes had only a secondary role in ion focusing properties. This fact was true for both the circular and noncircular samples tested.

Hexagonal holes. - The patterns eroded by the hexagonal holes are shown on figure 3(e). It is seen that ions were preferentially focused into the corners and away from the straight edges. The erosion ratios between sides and along the diagonals were about 7 and 14 percent larger than for the circular case, respectively. The increase in erosion ratio implies that for the same screen grid hole-to-hole spacing and operating conditions, the maximum accelerator web thickness is smaller for an array of hexagonal screen grid holes than for circular holes. The hexagonal holes therefore result in less operational flexibility than the circular holes. The possibility of increased open area of a hexagonal hole system might, however, compensate for the increase in erosion ratios over those of circular holes. Some of the variation of focusing properties noted for various hole shapes could be due to local variations of grid spacing during operation. Although the initial and final grid spacing were constant to within about 7 percent, it is possible that more variation in grid spacing was present during operation.

It was of interest to determine the relation between the angles in the screen holes and the angles of the eroded accelerator grid samples. These angles are described as θ_S and θ_A, respectively, and are shown on sketch B. The value of θ_A was taken to be that of the fringe area and in some cases was difficult to specify exactly due to the difficulty of determining the fringe edges. The values of θ_S and θ_A for the various samples are shown on table II along with the estimated uncertainty of the measurement. As indicated in table II, the uncertainty was estimated to be 5 degrees except where shown otherwise.

Square holes. - The patterns eroded by the square holes are shown in figure 3(f). As for the hexagonal holes, the ions were preferentially focused into the corners and away from the straight edges. The erosion ratios for the sides of the squares were about the same as for the circular holes. The erosion ratios along the diagonals were, however, about 36 and 6 percent larger than for the circular and hexagonal cases, respectively.

Triangular holes. - The triangular erosion patterns are shown on figure 3(g). As mentioned previously, the screen grid sample holes were inadvertently machined to a larger characteristic size than the other hole shapes. The erosion ratio from the center of symmetry of the triangle to the corner was over 0.9. This erosion ratio led to erosion patterns which were quite close to each other on the accelerator grid sample (fig. 3(g)). It is not known the extent to which the increase in the basic dimension impacted the focusing characteristics. It is likely, however, that the triangular pattern offers the least operational flexibility of all shapes tested.

Angle transformations. - It is possible that ion beamlets of various shapes other than circular would be desirable for some applications. For example, a beam deflection scheme (ref. 6) presently being studied for 5-cm thrusters uses electrostatic deflection. For ease of fabrication and to provide orthogonal deflection capability, the holes formed by the accelerator grid elements are square while, for present designs, the screen grid holes are round. Screen grid holes shaped such as to produce square ion beamlets might provide optimum beam deflection characteristics.

The data of Test II can be used to help determine the relation between screen hole shape and ion beamlet shape. The values of θ_A are plotted as a function of θ_S on figure 4 for the various screen hole shapes. The value of θ_A was less than θ_S except in the circular case for which both angles are at 180°. The data of figure 4 indicate that ion beamlets with 90° angles would be produced from screen grid holes with angles of about 140°. In addition, as seen from figure 3, the screen grid holes should be curved.

Test III

This test was essentially a repeat of Test II with the ion beam current increased to a value nearer the Child's law current limit of the grid system. Operation near the current limit should lead to maximum ion beam spreading in the accelerator region, and hence, maximum estimates of ion erosion ratios.

The value of the Child's law limit for the entire grid system was obtained by plotting the ratio of the impingement current to the ion beam

current as a function of total extraction voltage (ref. 11). The results indicated that the minimum total extraction voltage for 0.75 A ion beam current to avoid significant direct ion impingement was about 3400 volts. The values of 2000 and -1330 volts were selected the screen and accelerator grids, respectively, so that the thruster was operated very close to the Child's law limit ion current of the grid system.

The shapes of the erosion patterns for the various screen-grid holes were essentially the same as in Test II and will not be shown. The values of the erosion ratios and of θ_S and θ_A are given in table II.

Circular holes. - The erosion ratio for the circular case (table II) increased by about 28 percent over that of Test II. For real applications, grids would normally be operated at a lower fraction of the Childs law limited current than that of Test III. An erosion ratio of about 0.65 should then represent an approximate upper limit for conservative grid design.

Hexagonal holes. - The erosion ratios for the hexagonal holes were less than for the circular holes in both directions. In fact, the erosion ratio of Test III actually decreased from those measured in Test II. The reason for this decrease is not known. It is possible that local buckling caused a change in the grid to grid spacing in the region of the hexagonal hole sample and led to a decrease in ion beam spread in the accelerator region.

Square holes. - The erosion ratios parallel to the sides and along the diagonals increased for Test III by about 2 and 9 percent, respectively, from those of Test II. Along the diagonals the erosion ratio was about 16 percent larger than the erosion ratio for the circular holes. Such data indicate that square holes are limited to a smaller operating range than circular holes.

Triangular holes. - The erosion ratios for the triangular hole samples are shown in table II. The erosion ratios were equal for Test II and Test III. As indicated previously, the erosion ratios were of such magnitude that triangular holes are probably undesirable for this application.

Test IV

Another test was made to determine if square shaped ion beamlets could be produced from easily fabricated screen grid holes. The use of square ion beamlets could be of interest for the electrostatic beam deflection scheme described previously.

From the previous tests (fig. 4) it was determined that ion beamlets with 90° angles would be formed from screen grid holes which had angles

of about 140°. In addition, straight edges were avoided on the screen grid holes because such edges produced a bow in the accelerator grid hole (fig. 3). To satisfy these conditions, screen grid holes of a shape shown in sketch F were fabricated. The characteristic dimension $2R_S$ was selected as 5.0 mm, which was the nominal dimension of the previous samples. The electrodes used to electric discharge machine the screen grid holes were fabricated from square stock 5.0 mm on a side. The electrode was then turned on a lathe off center a distance ℓ on all four sides to a radius γ. In general, the relation between the desired minimum dimension $2R_S$ and the angle θ_S is given by

$$\ell = \frac{R_S}{\frac{\sin(\pi/4)}{\cos(\theta_S/2)} - 1} \tag{1}$$

$$\gamma = \ell + R_S \tag{2}$$

The values of ℓ and γ were selected to produce screen sample angles (θ_S) between about 121° and 140°. Four samples were made (A to D) and the values of R_S, D_S, and θ_S for all samples are shown in table II.

The eroded accelerator samples for the various screen grid samples of Test IV are shown in figure 5. The values of the erosion ratios and θ_A are given in table II. The eroded areas from sample A were very nearly square in shape. In addition, the erosion ratios were close to those of the circles and hexagons of the previous test. Samples B and C produced holes less square than sample A. Sample C was made with a larger characteristic dimension than the other three samples. It is seen in table II that the increased size increased the erosion ratios. This indicates that specification of the exact screen grid hole design to produce a specific beamlet shape is a function of the ratio of screen grid hole dimension to grid-grid spacing. Sample D, which had the largest radius of curvature produced holes with the smallest values of θ_A, as expected. The erosion ratios were about equivalent to those of samples A and B.

Test V

It was seen in previous tests (figs. 2 and 5(a)) that small irregularities occurred in the holes in the accelerator grid sample. Test V was made in order to determine the effect of various defects in the screen grid holes on the ion focusing characteristics. Defects were placed on four screen grid samples (E to H). The defects consisted of indentations cut into and protuberances extended from the edges of circular holes. The protuberances and indentations were made both pointed and rounded in shape. In addition, wires and metal bands were extended completely across the holes. Figures 6(a) and (b) show the defects

added to samples E and H. The accelerator grid samples produced by screen samples E and H are shown in figures 6(c) and (d). The effect of a protuberance on the screen hole was to produce a protuberance in the corresponding accelerator grid hole of about the same length. The protuberance produced was rounded for all samples tested. The effect of an indentation on the edge of a screen hole was to produce a large indentation on the accelerator grid hole. The erosion pattern extended beyond the normal fringe area between 1 to 1.5 times the depth of the indentation as seen in figures 6(c) and (d). The wires and bands across the holes produced a widely split beamlet with very little dependence on the width of the band (except for bands which were so wide that they covered up a large fraction of the screen hole).

CONCLUDING REMARKS

Tests were made to determine the ion focusing characteristics of circular, hexagonal, square, and triangular screen-grid holes. The focusing was found to be dependent on both the thruster operating conditions and the screen grid hole shape and size. The circular hole shape had the lowest erosion ratios followed in increasing order by the hexagonal, square, and triangular shapes. The increase possible in open area of the noncircular holes could, however, compensate for the increases in erosion ratios. The hexagonal hole shape appeared to be the most promising noncircular hole shape for high open area grids. Inspection of the erosion patterns provided a correlation between the shapes of the screen grid holes and the ion beamlet shape in the region of the accelerator grid. This correlation was used to produce square ion beamlets which could be of interest for an electrostatic beam deflection scheme. The effect of various defects in the screen grid was also investigated.

REFERENCES

1. Bartz, Donald R.; and Horsewood, J. L.: Characteristics, Capabilities, and Costs of Solar Electric Spacecraft for Planetary Missions. J. Spacecraft Rockets, vol. 7, no. 12, Dec. 1970, pp. 1379-1390.

2. Strack, William C.; and Hrach, Frank J.: Early Application of Solar-Electric Propulsion to a 1-Astronomical-Unit Out-of-the-Ecliptic Mission. NASA TN D-5996, 1970.

3. Kerrisk, D. J.; and Kaufman, H. R.: Electric Propulsion Systems for Primary Spacecraft Propulsion. Paper 67-424, AIAA, July 1967.

4. Bechtel, Robert T.: Discharge Chamber Optimization of the SERT II Thruster. J. Spacecraft Rockets, vol. 5, no. 7, July 1968, pp. 795-800.

5. King, H. J.; Poeschel, R. L.; and Ward, J. W.: A 30-cm, Low-Specific-Impulse, Hollow-Cathode, Mercury Thruster. J. Spacecraft Rockets, vol. 7, no. 4, Apr. 1970, pp. 416-421.

6. Collett, C. R.; King, H. J.; and Schnelker, D. E.: Vectoring of the Beam from Ion Bombardment Thrusters. Paper 71-691, AIAA, June 1971.

7. King, H. J.; and Poeschel, R. L.: Low Specific Impulse Ion Engine. Hughes Research Labs. (NASA CR-72677), Feb. 1970.

8. Lathem, Walter C.: Effects of Electrode Misalinement in Kaufman Thrusters. J. Spacecraft Rockets, vol. 5, no. 6, June 1968, pp. 735-737.

9. Sohl, Gordon; and Fosnight, Verryl V.: Thrust Vectoring of Ion Engines. J. Spacecraft Rockets, vol. 6, no. 2, Feb. 1969, pp. 143-147.

10. Masek, T. D.; and Pawlik, E. V.: Thrust System Technology for Solar Electric Propulsion. Paper 68-541, AIAA, June 1968.

11. Kerslake, William R.: Accelerator Grid Tests on an Electron-Bombardment Ion Rocket. NASA TN D-1168, 1962.

TABLE I. - THRUSTER OPERATING PARAMETERS

Test	Screen		Accelerator		Spacing, L, mm
	V	A	V	A	
I	2600	0.42	870	0.010	3.52±0.3
II	2000	.54	1220	.010	4.1±0.3
III	2000	.75	1330	.011	4.1±0.3
IV	2000	.40	1330	.006	4.1±0.3
V	2000	.55	1330	.005	4.1±0.3

TABLE II. - GEOMETRY OF SCREEN AND ACCELERATOR HOLES

Test	Screen hole geometry	R_S, mm	D_S, mm	$\frac{R_A}{R_S}$	$\frac{D_A}{D_S}$	θ_S, deg	θ_A, deg±5
I	Circle	2.5	2.5	0.45	0.45	180	180
II	Circle	2.5	2.5	0.50	0.50	180	180
	Hexagon	2.5	2.8	.57	.64	120	55
	Square	2.5	3.5	.49	.68	90	43
	Triangle	2.9	5.7	.63	.91	60	33±10
III	Circle	2.5	2.5	0.64	0.64	180	180
	Hexagon	2.5	2.8	.55	.62	120	74
	Square	2.5	3.5	.51	.74	90	49
	Triangle	2.9	5.7	.66	.91	60	27±10
IV	Curve A	2.3	2.6	0.57	0.67	139±3	79
	Sided B	2.2	2.5	.51	.64	134±3	76
	Squares C	2.4	2.9	.64	.75	136±3	78
	D	2.3	2.5	.53	.64	121±3	67

E-6558

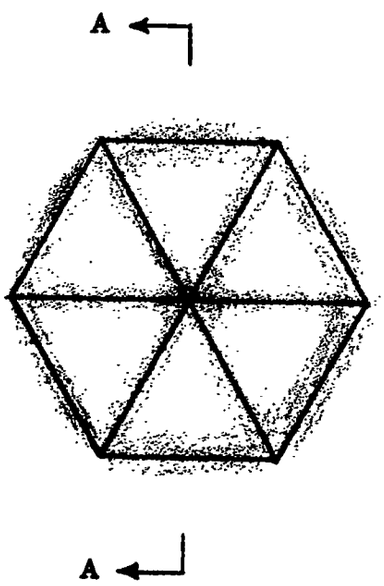

Upstream face

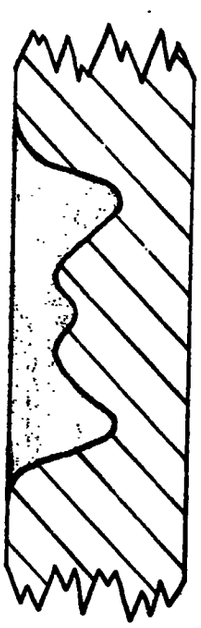

Section view A-A

Sketch A

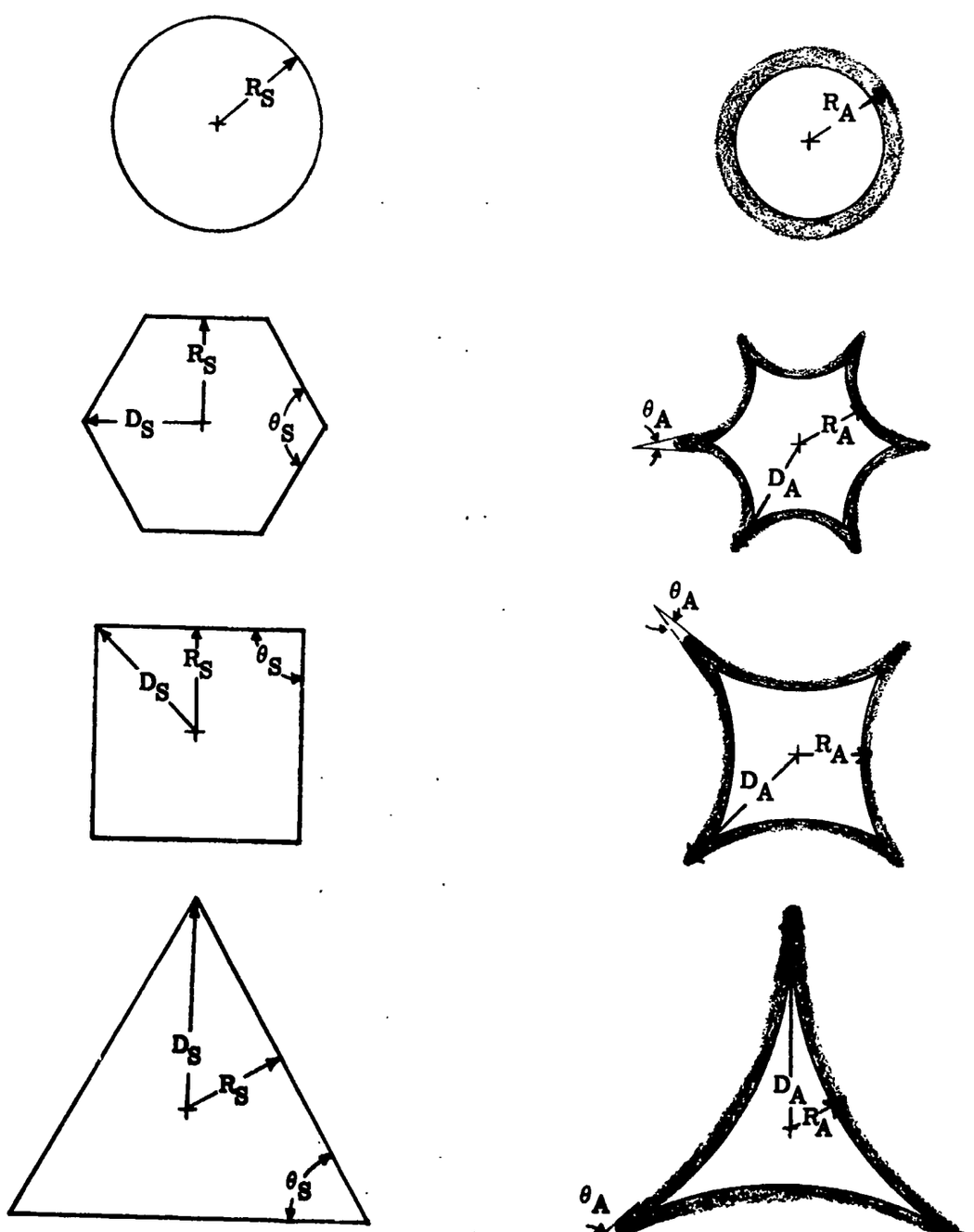

Screen samples

Resultant accelerator samples

Sketch B

E-6558

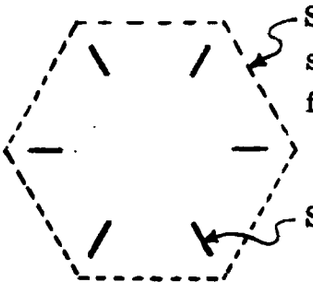

Sketch C

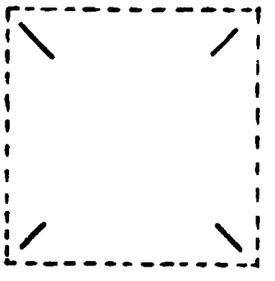

Sketch D

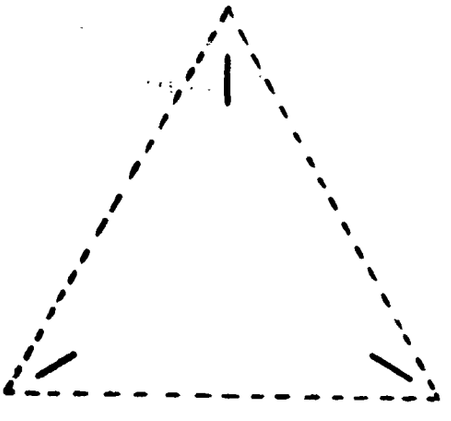

Sketch E

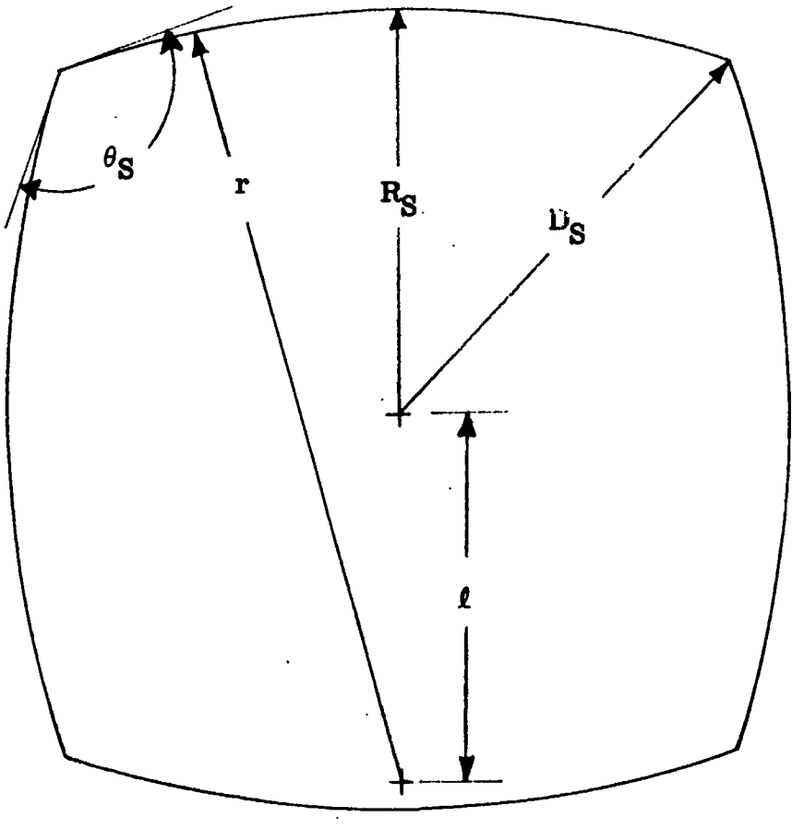

Sketch F

E.-6558

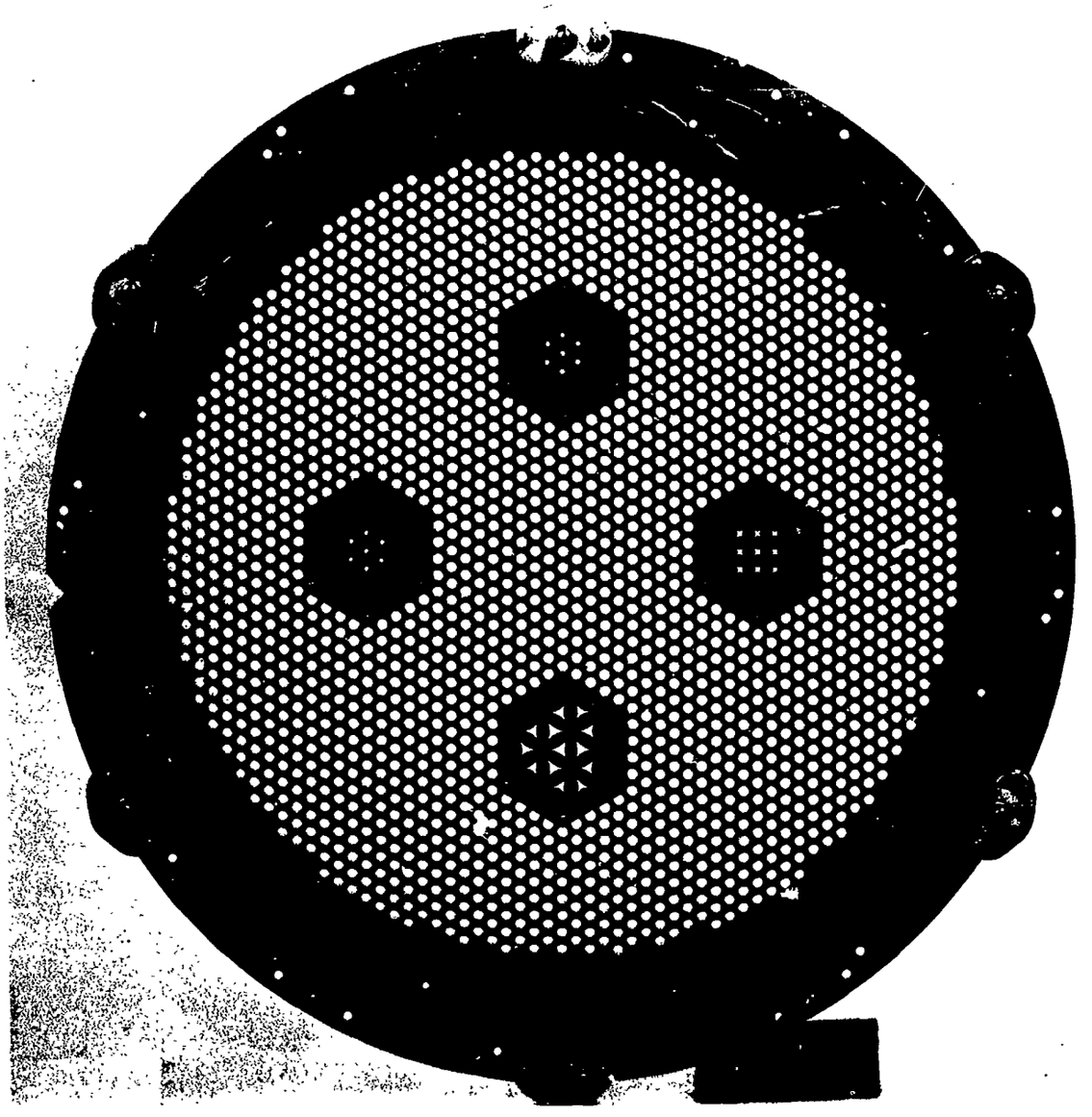

Figure 1. - Upstream view of accelerator grid system after Test II.

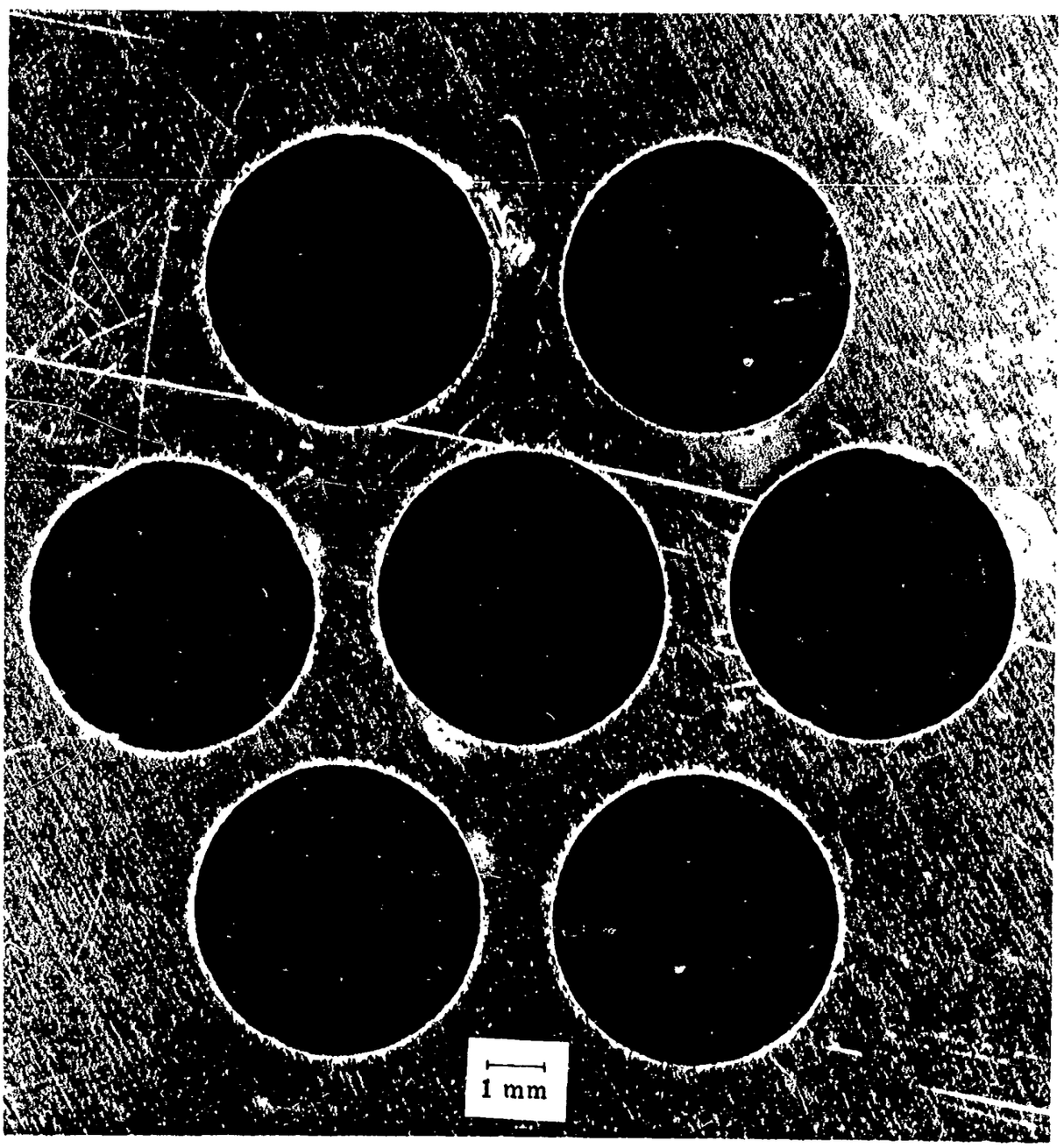

(a) Circular hole screen grid sample.

Figure 2. - Screen and accelerator grid samples from Test I.

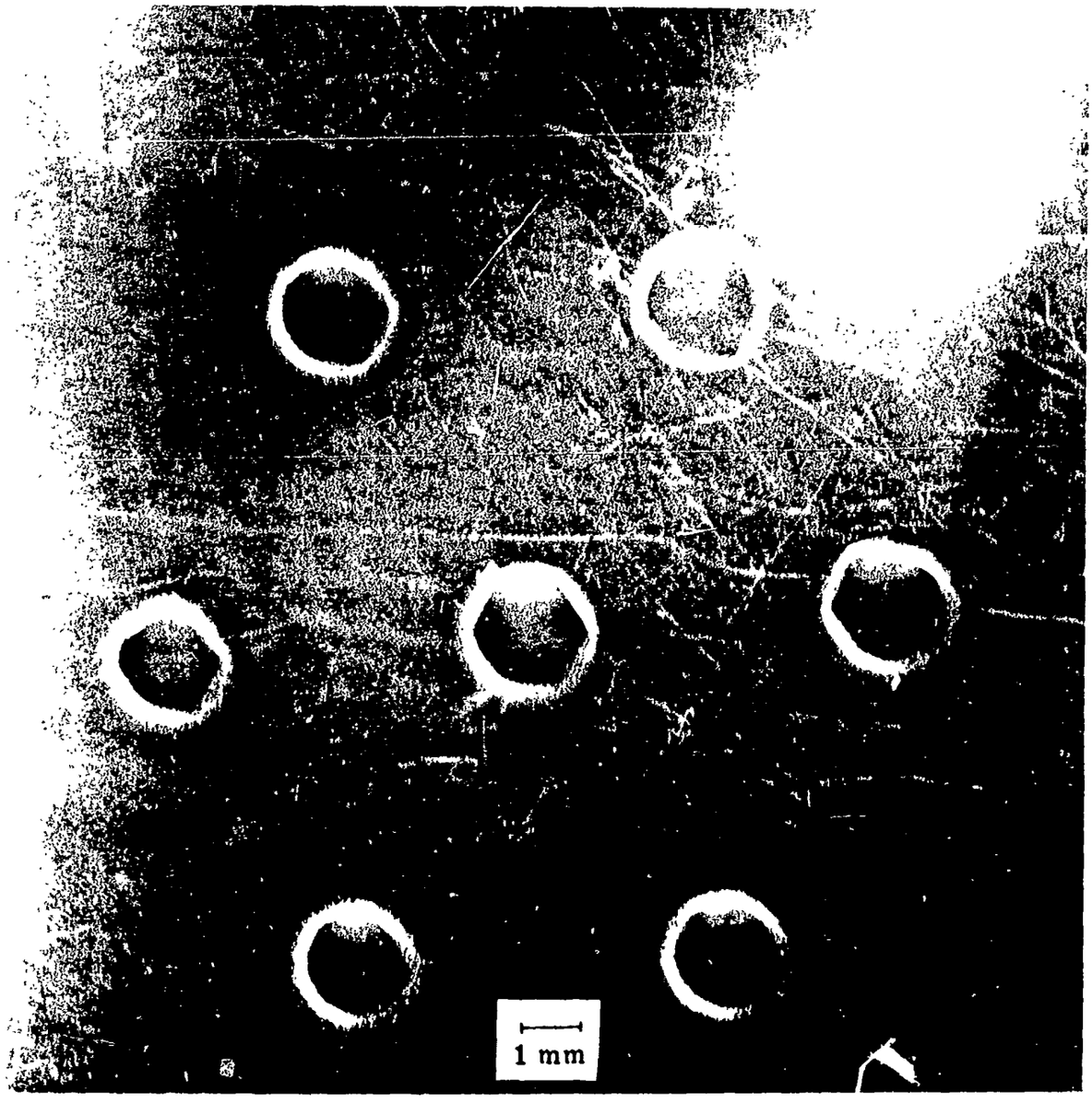

(b) Erosion produced by circular hole screen grid sample.

Figure 2. - Concluded.

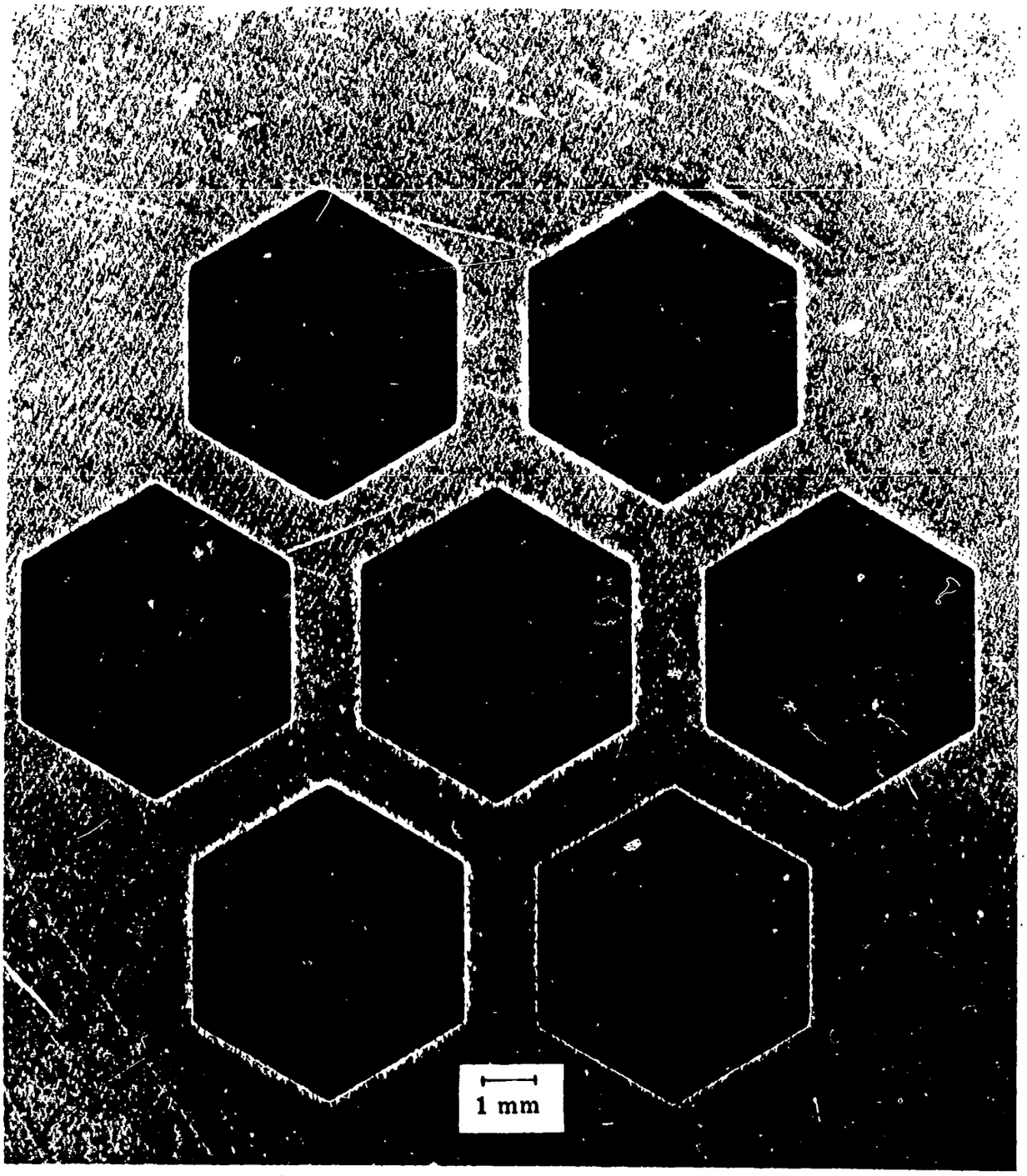

(a) Hexagonal hole screen grid sample.

Figure 3. - Screen and accelerator grid samples from Test II.

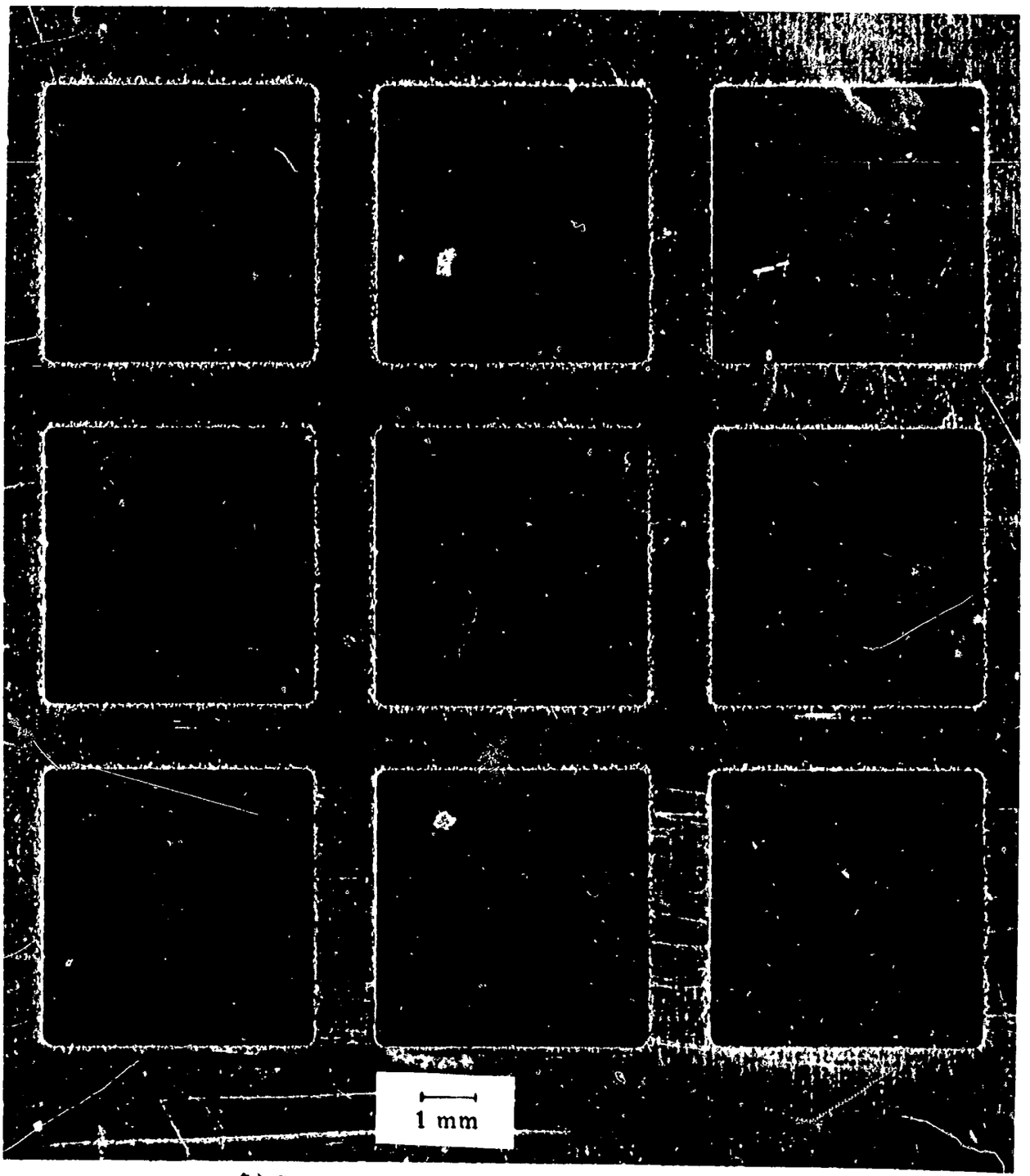

(b) Square hole screen grid sample.

Figure 3. - Continued.

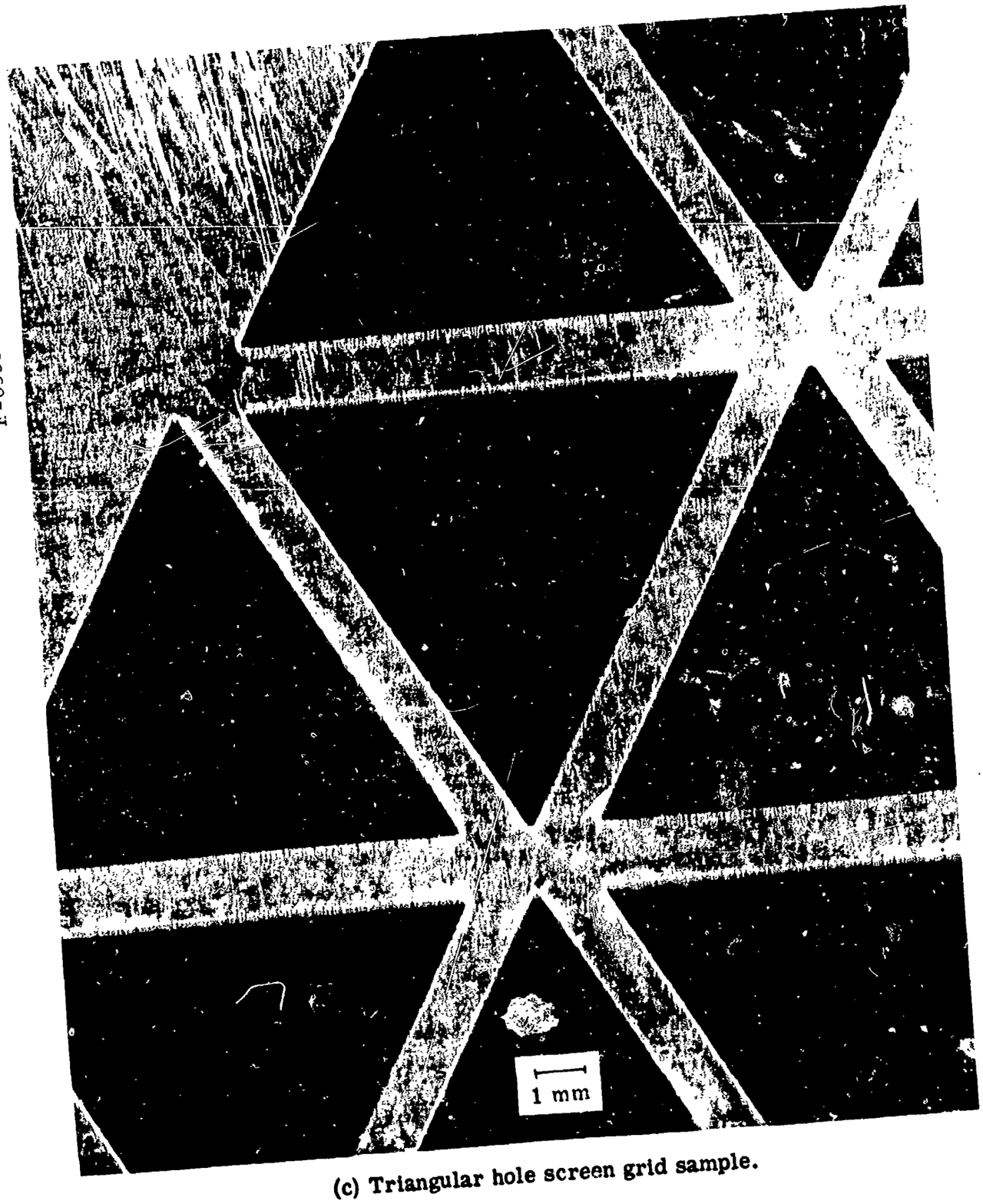

(c) Triangular hole screen grid sample.

Figure 3. - Continued.

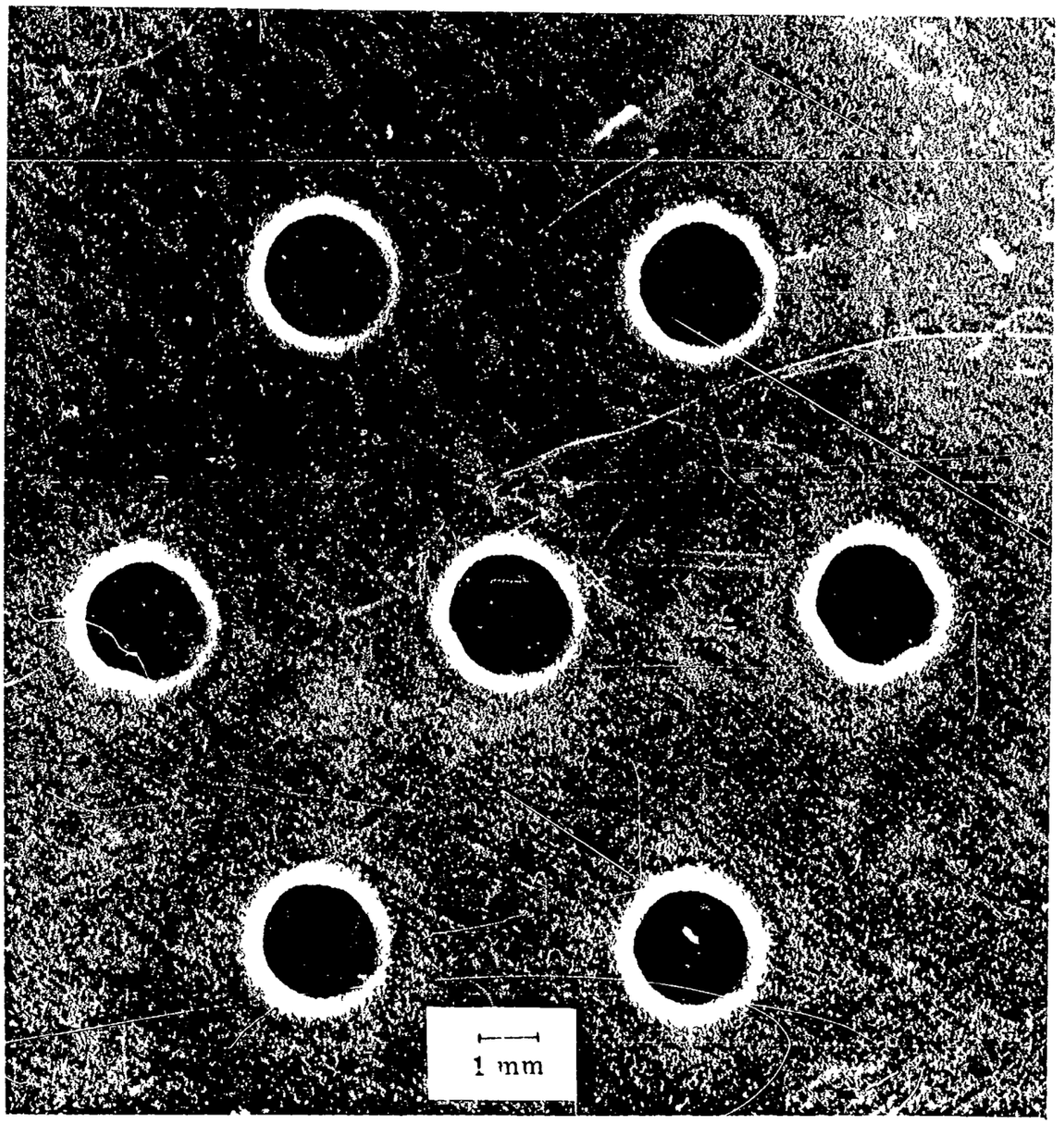

(d) Erosion produced by circular hole screen grid sample.

Figure 3. - Continued.

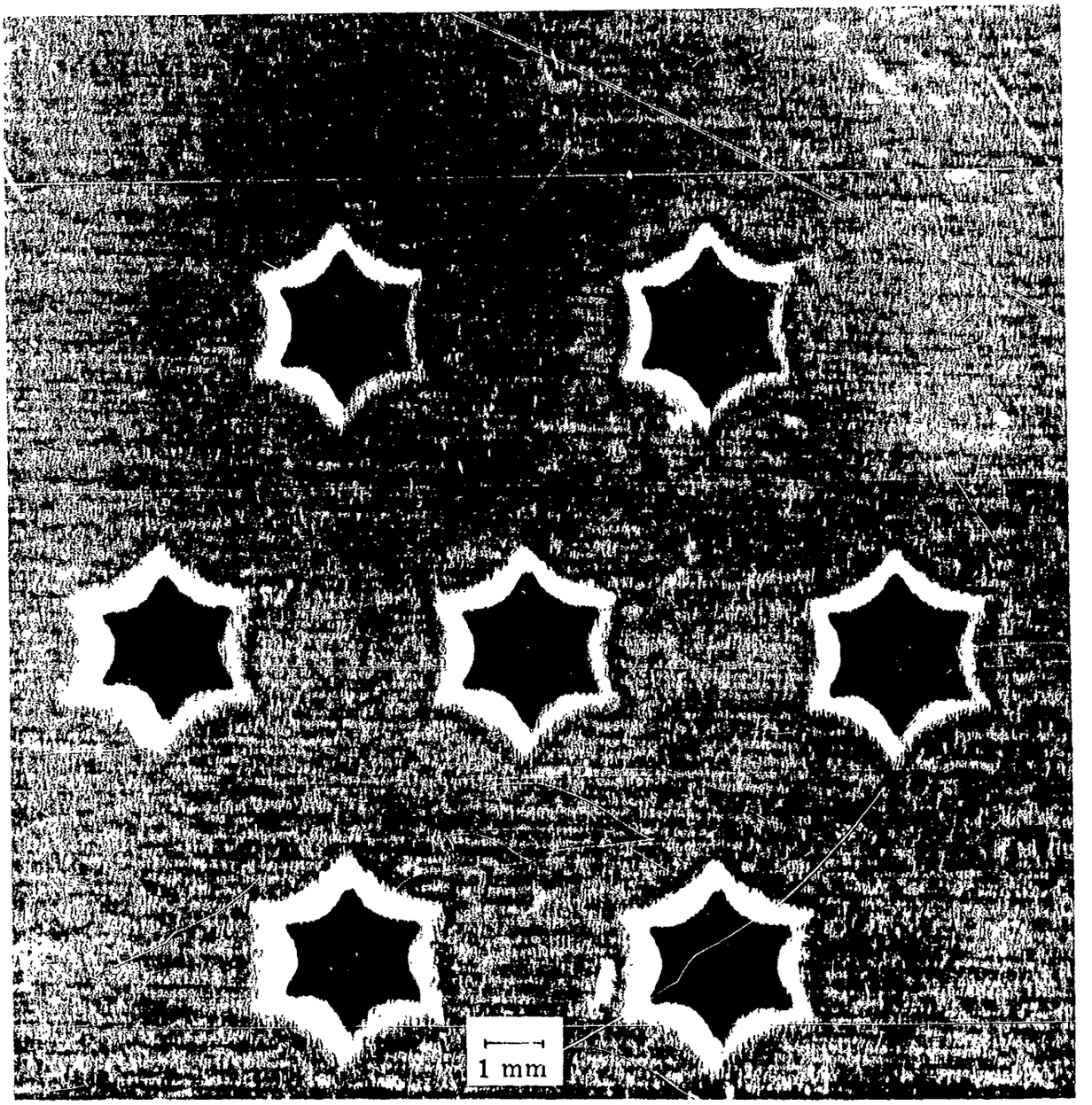

E-6552

(e) Erosion produced by hexagonal hole screen grid sample.

Figure 3. - Continued.

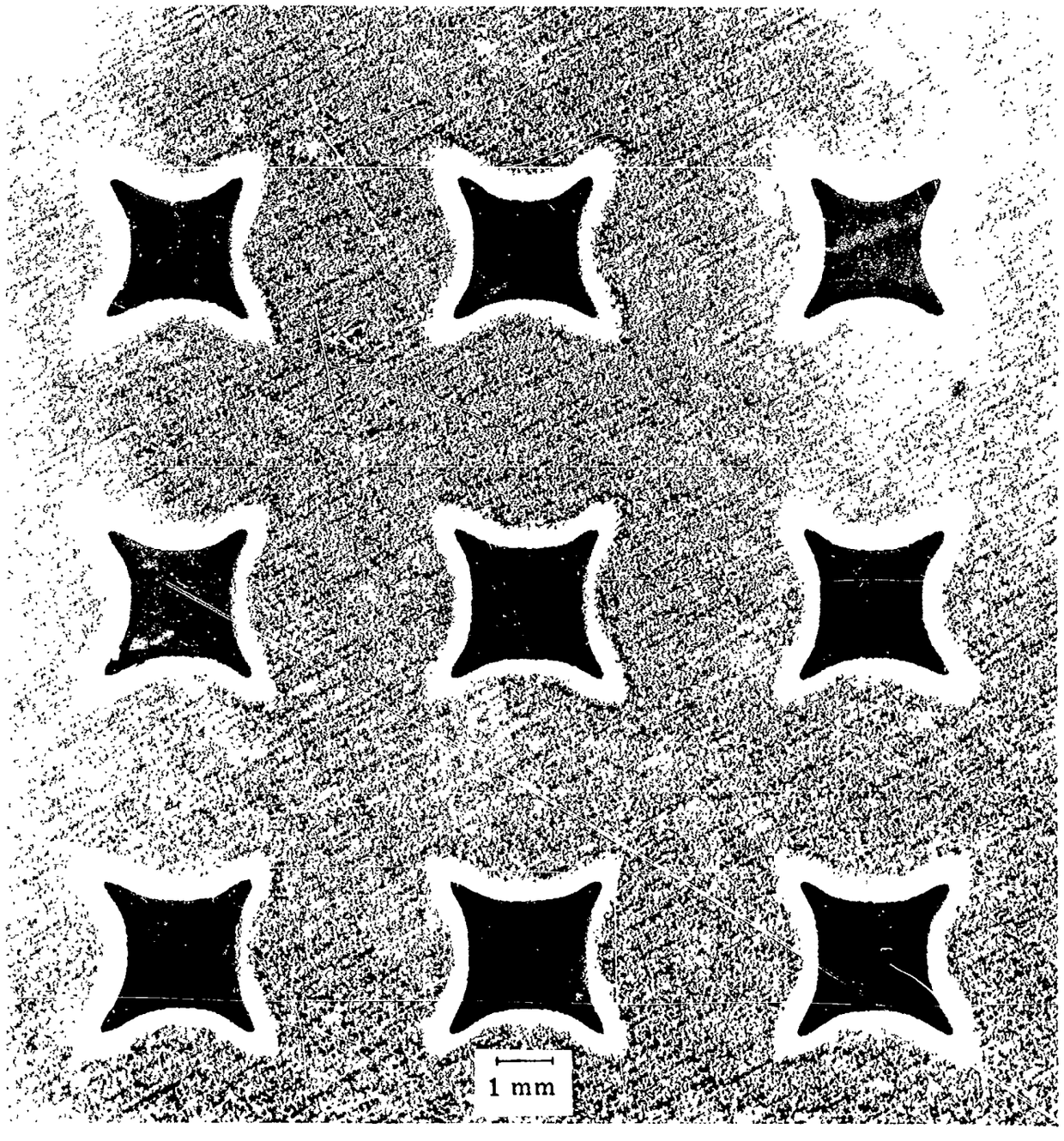

(f) Erosion produced by square hole screen grid sample.

Figure 3. - Continued.

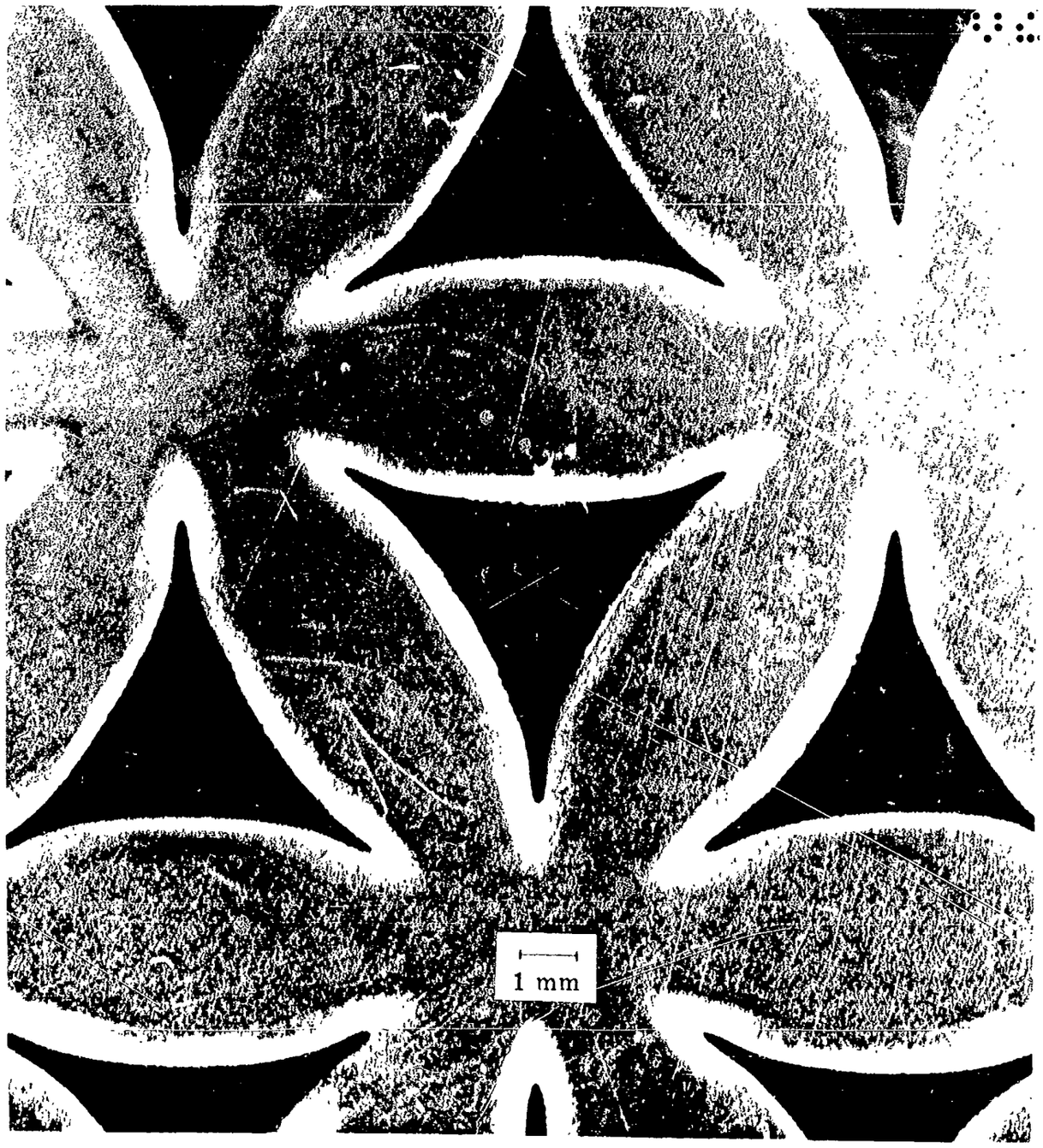

(g) Erosion produced by triangular hole screen grid sample.

Figure 3. - Concluded.

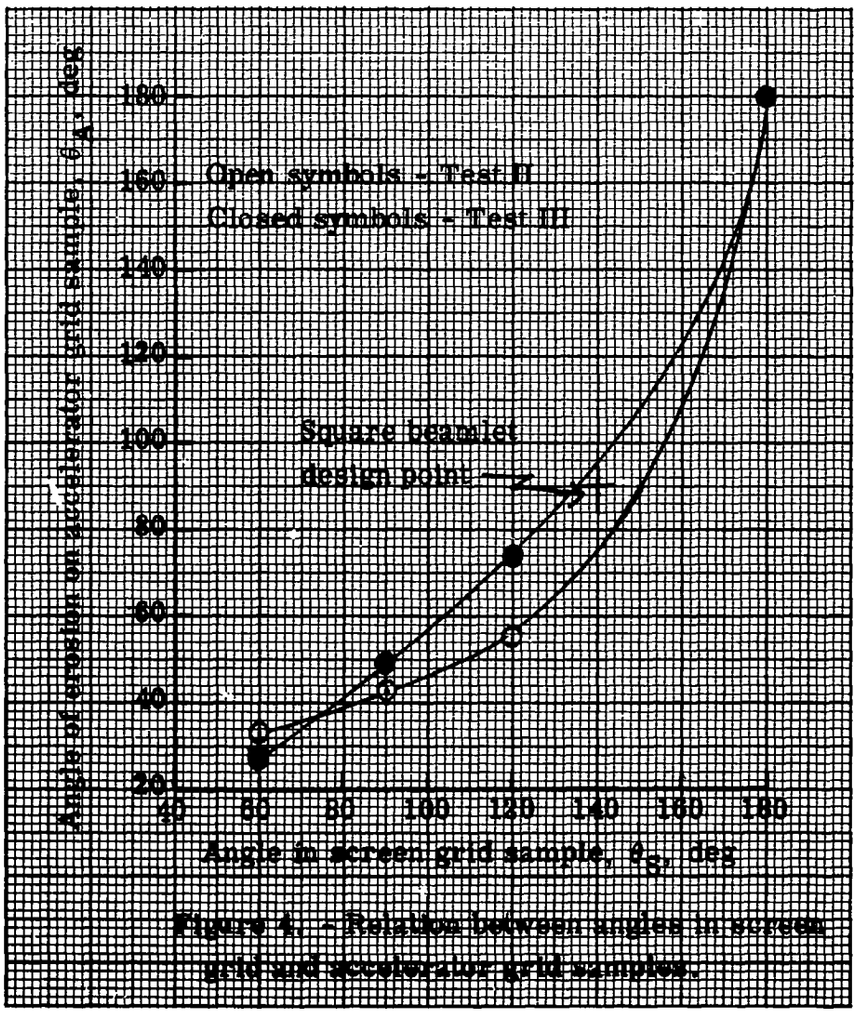

Figure 4. - Relation between angles in screen grid and accelerator grid samples.

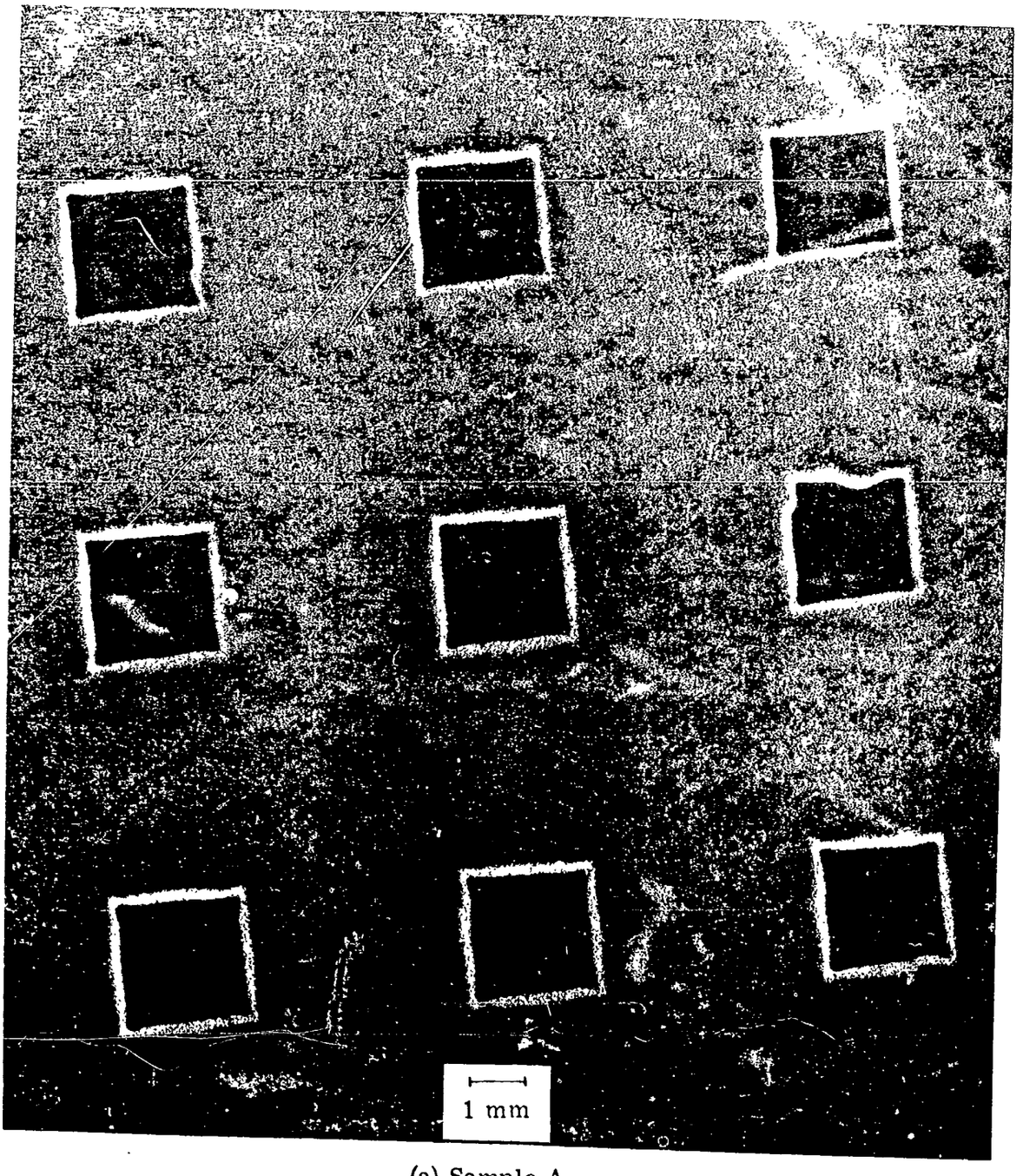

(a) Sample A.

Figure 5. - Accelerator grid samples after Test IV.

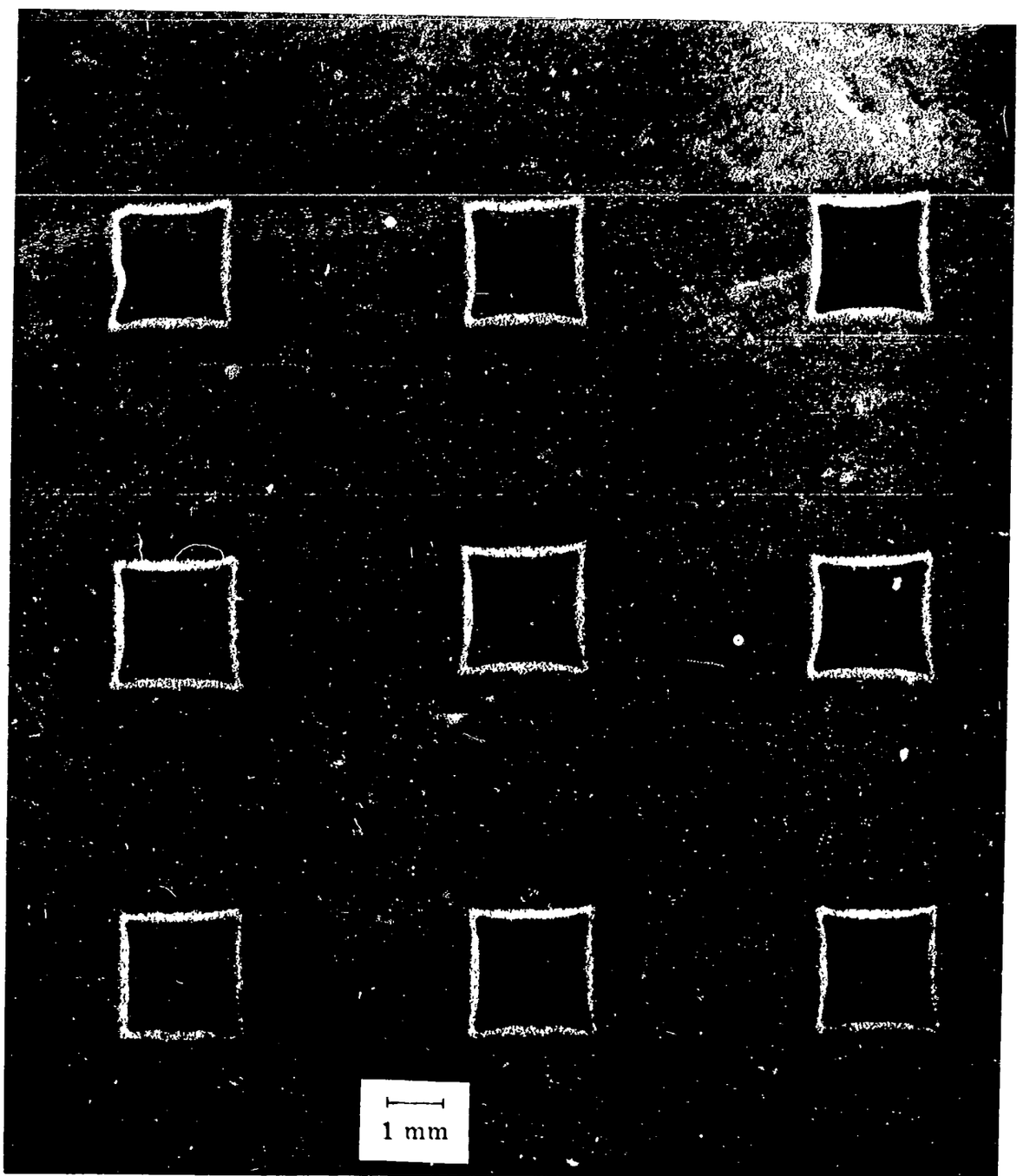

(b) Sample B.

Figure 5. - Continued.

E-6558

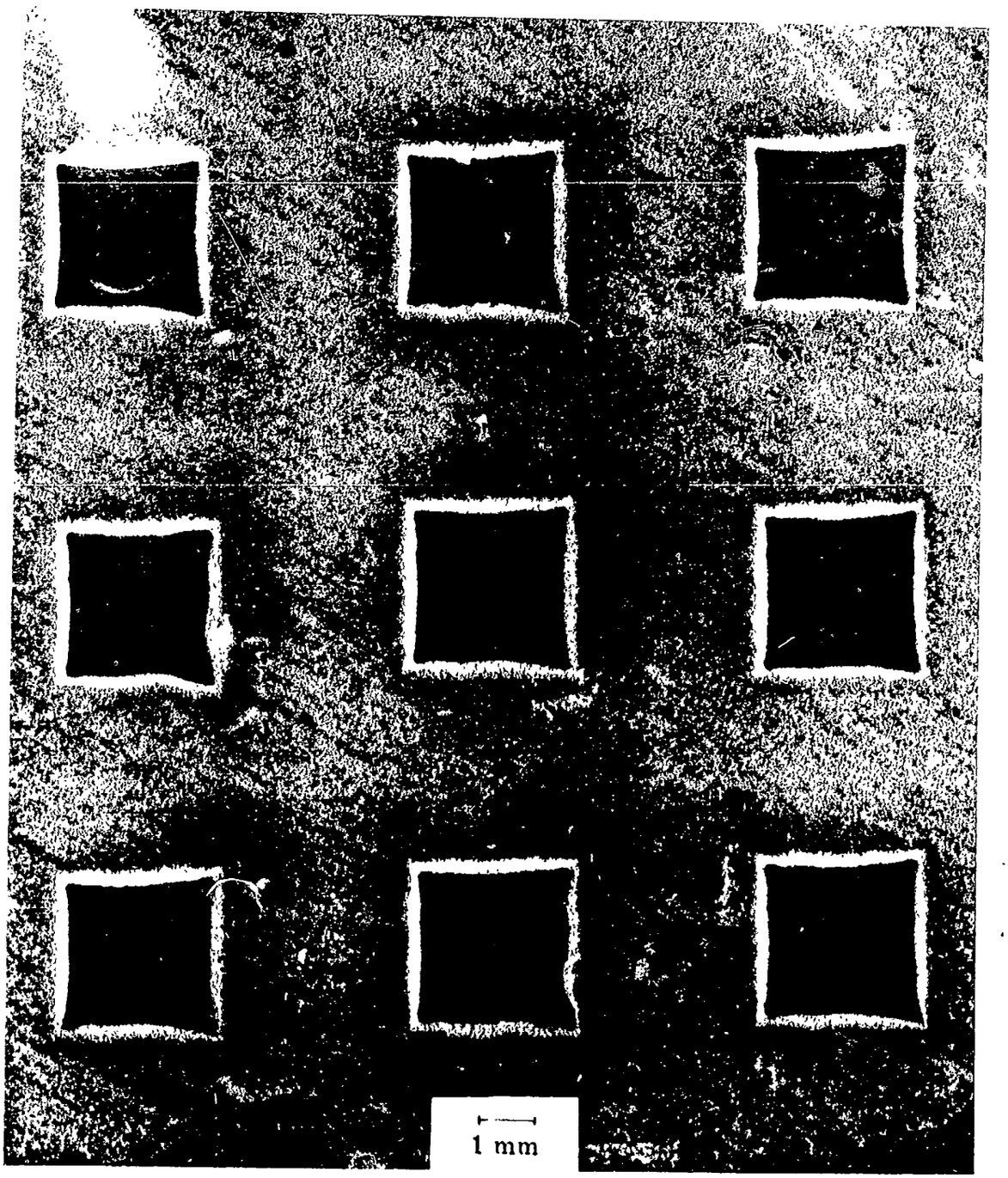

(c) Sample C.

Figure 5. - Continued.

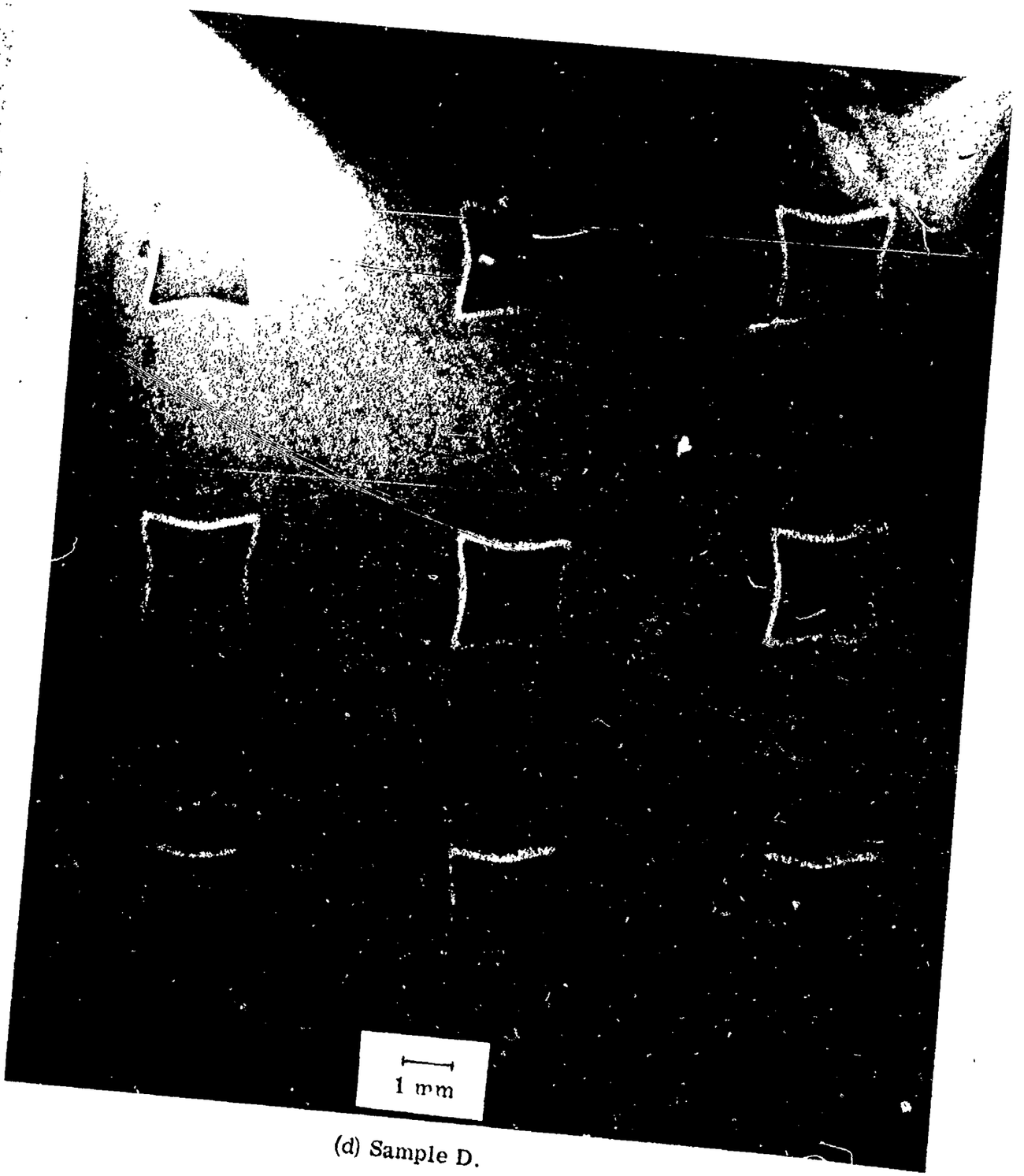

(d) Sample D.

Figure 5. - Concluded.

E-6559

(a) Screen grid sample E.

Figure 6. - Screen and accelerator grid samples from Test V.

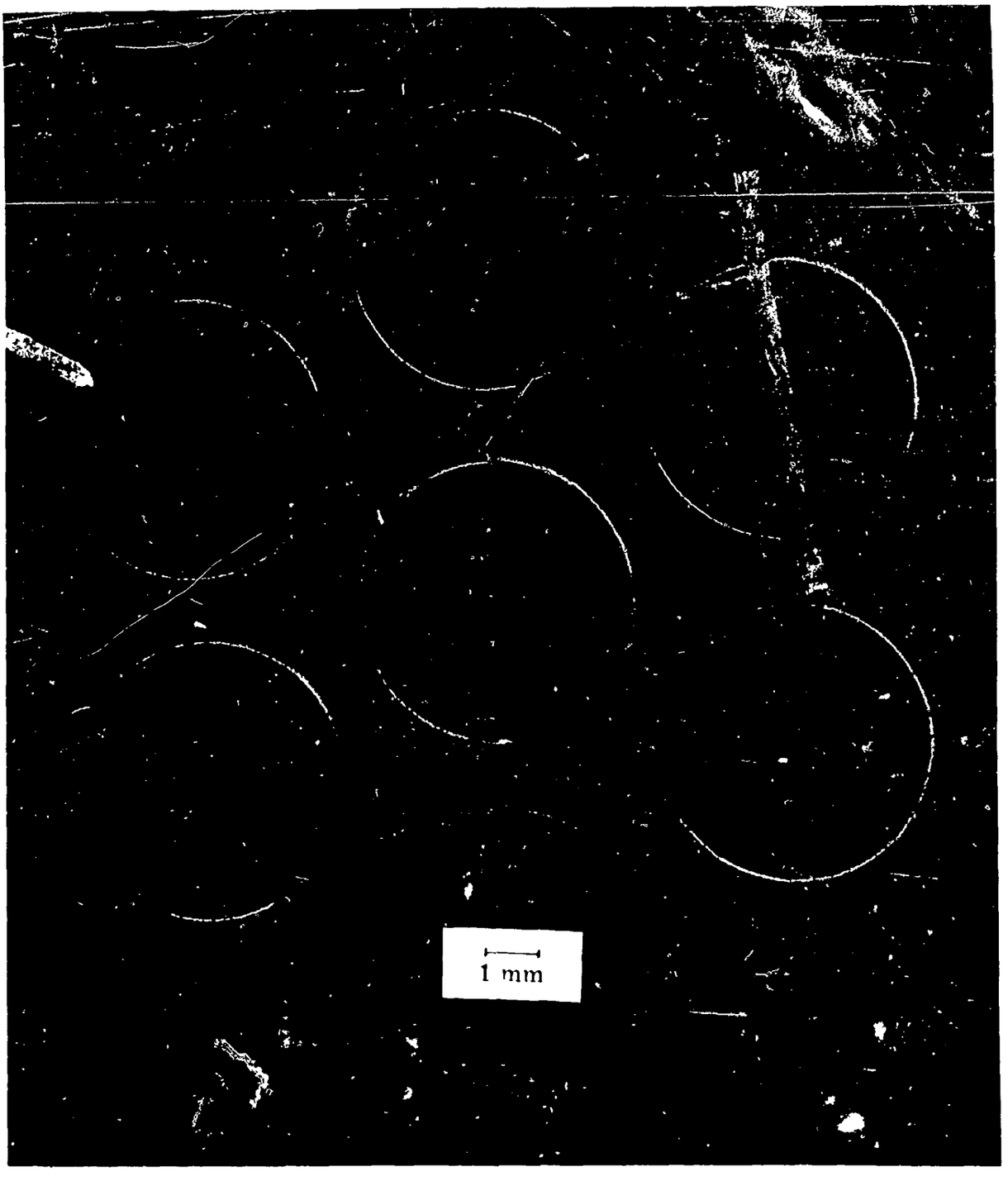

(b) Screen grid sample H.

Figure 6. - Continued.

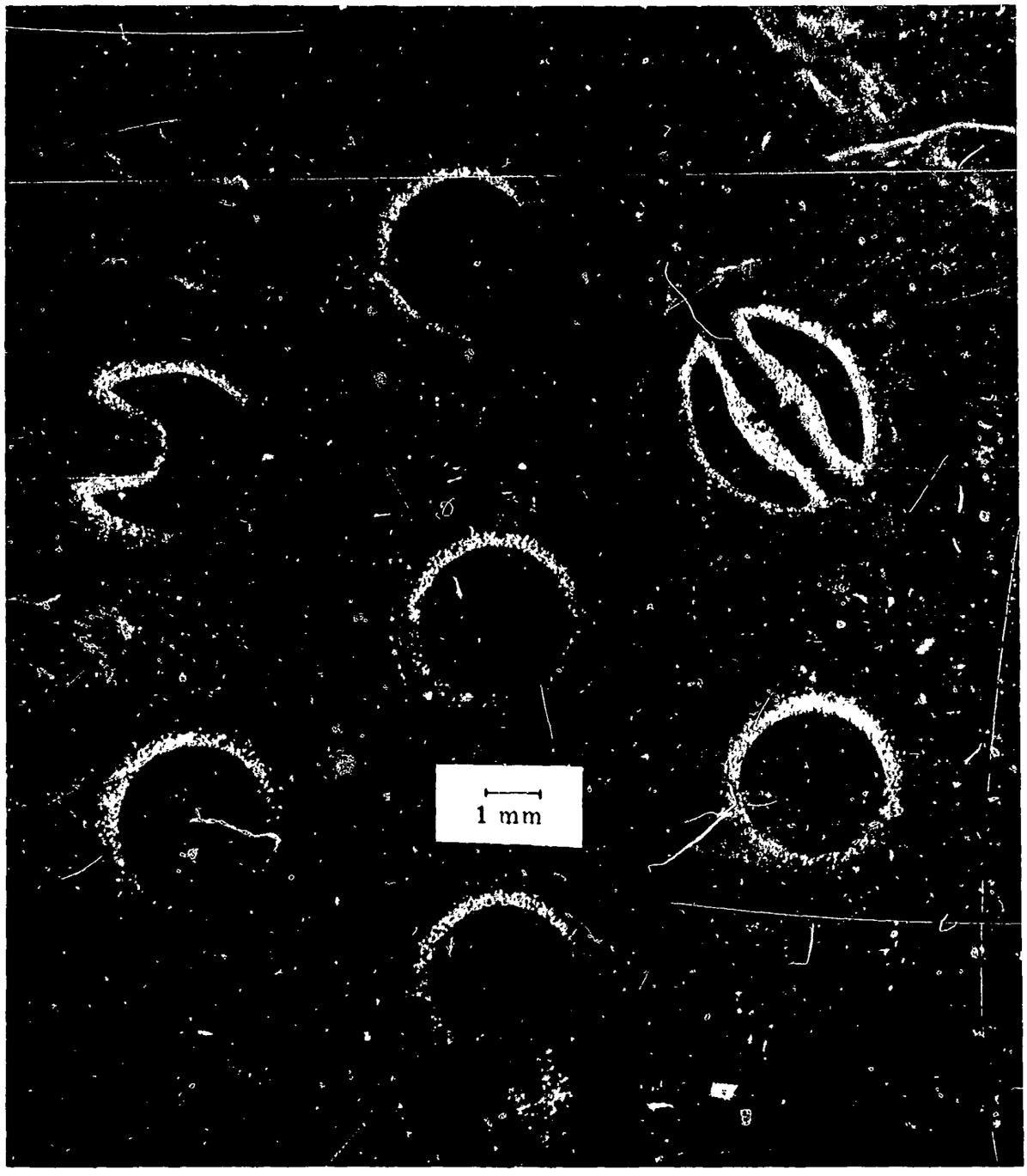

(c) Accelerator grid sample E.

Figure 6. - Continued.

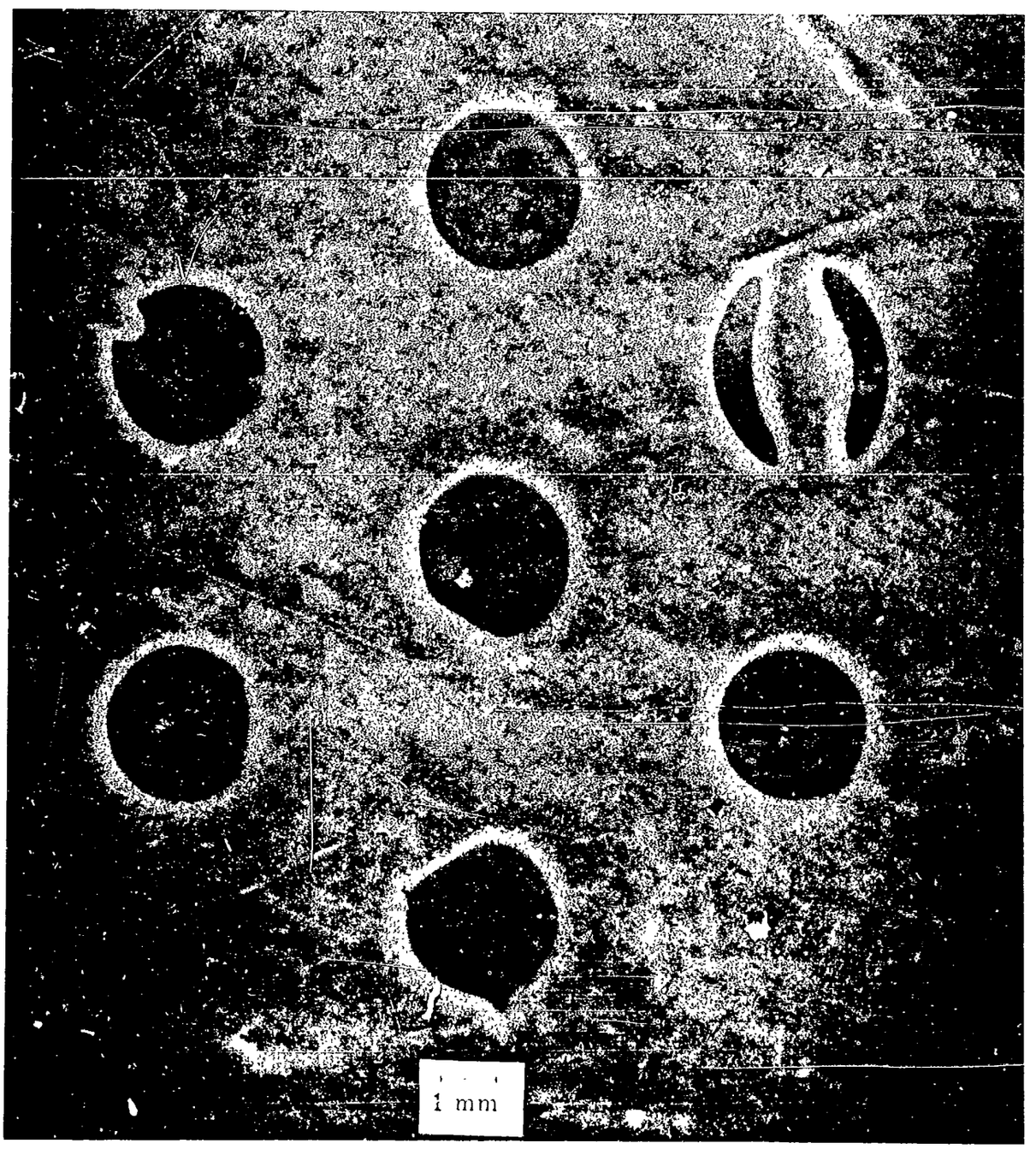

(d) Accelerator grid sample H.

Figure 6. - Concluded.